Food Hydrocolloids 71 (2017) 26–34

Contents lists available at ScienceDirect

Food Hydrocolloids

journal homepage: www.elsevier.com/locate/foodhyd

Cassava starch films containing rosemary nanoparticles produced by solvent displacement method

Alex López-Córdoba [a, *], Carolina Medina-Jaramillo [a, b], Danyxa Piñeros-Hernandez [a], Silvia Goyanes [a, **]

[a] Universidad de Buenos Aires, Facultad de Ciencias Exactas y Naturales, Departamento de Física, Laboratorio de Polímeros y Materiales Compuestos (LP&MC), Instituto de Física de Buenos Aires (IFIBA-CONICET), Buenos Aires, Argentina
[b] Universidad de Buenos Aires, Facultad de Ingeniería, Instituto de Tecnología en Polímeros y Nanotecnología (ITPN-CONICET), Buenos Aires, Argentina

ARTICLE INFO

Article history:
Received 14 January 2017
Received in revised form
24 April 2017
Accepted 25 April 2017
Available online 27 April 2017

Keywords:
Edible films
Cassava starch
Rosemary
Nanoparticles
Antioxidant activity
Packaging

ABSTRACT

Cassava starch films containing rosemary nanoparticles were successfully produced using a simple approach. Different concentrations (5 and 20% w/w) of ethanolic extracts of rosemary were added to the film-forming aqueous blends containing cassava starch and glycerol, and in this way, rosemary nanoparticles were produced by the solvent displacement. The formulations added of the lowest extract amount led to films containing well distributed rosemary nanoparticles within the matrix. In contrast, higher extract concentration provoked the formation of agglomerates of nanoparticles within the films. Fourier transform infrared spectroscopy and thermogravimetric analysis suggested that the availability of hydroxyl groups within the starch matrix was decreased due to the presence of the rosemary-related compounds. Tensile properties of the cassava starch films were also influenced by the addition of rosemary extract. It was found that the rosemary nanoparticles were able to act as a reinforcement of the starch matrix increasing the elastic modulus and the tensile strength of the films up to 4.0-fold and 2.5-fold, respectively; while the strain at break was slightly decreased, compared with the control films. Finally, the release kinetics of rosemary polyphenols from cassava starch active films to aqueous and fatty food simulants was analyzed. In the aqueous medium, all active films released a polyphenols amount above 60% within the first hour of assay. In contrast, the release rate of rosemary polyphenols into ethanol (i.e. a fatty food simulant) was slower compared with the aqueous one.

1. Introduction

Packaging materials plays an important role in containing and preserving foods throughout the supply chain. The most frequently used packaging materials are based on polymers from non-renewable sources, which are associated with environment concerns. Therefore, several researches performed in the last years deal with the development of new food packaging based on natural polymers such as starch, cellulose, gelatin, alginates, among others. Between them, starch has been considered as one of the most promising candidates for future materials because of its biodegradability, low price, abundance, and thermoplastic behavior (García, Famá, D'Accorso, & Goyanes, 2015; Jiménez, Fabra, Talens, & Chiralt, 2012).

Food packaging can be termed active when it performs certain desirable role other than providing inert barrier to external conditions (Bhushani & Anandharamakrishnan, 2014). Active packaging systems could include antioxidants, antimicrobial agents or oxygen scavengers (Chang-Bravo, López-Córdoba, & Martino, 2014; Fabra, López-Rubio, & Lagaron, 2016; Piñeros-Hernandez, Medina-Jaramillo, López-Córdoba, & Goyanes, 2017). These substances can be naturally or synthetically derived, although consumers generally prefer those materials from natural sources. Other than these, moisture absorbing, flavor or odor absorbing active packaging systems are also being developed for food applications (Bhushani & Anandharamakrishnan, 2014).

Rosemary (*Rosmarinus officinalis* L.) leaves constitute a rich source of antioxidant compounds, which could be potentially used as additives in foods or food packagings (Piñeros-Hernandez et al.,

* Corresponding author.
** Corresponding author.
E-mail addresses: alexlcordoba@gmail.com (A. López-Córdoba), goyanes@df.uba.ar (S. Goyanes).

http://dx.doi.org/10.1016/j.foodhyd.2017.04.028
0268-005X/

2017). Several studies have demonstrated that the addition of rosemary extract into food products, such as processed meat and processed fish and fishery products, slows down or prevents the oxidation reaction (Aguilar et al., 2008; Ribeiro et al., 2016). Among their constituents, the most abundant individual antioxidant components in rosemary are rosmarinic acid (i.e. a water-soluble phenolic acid) and carnosic acid (i.e. an oil-dispersible diterpenoid) (Fig. 1).

Solvent extraction is the method commonly used for the extraction of rosemary active compounds. Recent investigations are focused on the use of green solvents accepted in the food industry, such as water and ethanol (Ribeiro et al., 2016; Rodríguez-Rojo, Visentin, Maestri, & Cocero, 2012). It has been reported that the differences of solvent polarity allowed obtain extracts with different chemical composition. For instance, Rodríguez-Rojo et al. (2012) worked on the extraction of antioxidants from rosemary with ethanol and water as solvents and determined the concentration of main bioactive compounds present in the rosemary extracts (carnosic acid and rosmarinic acid) by high performance liquid chromatography (HPLC). These authors found that the aqueous extracts showed higher concentration of rosmarinic acid compared with the ethanolic extracts; however, the concentration of carnosic acid was below the detection limit (0.0035 mg/mL). In contrast, the rosemary extracts obtained using ethanol were richer in carnosic acid (0.36 mg/mL) than in rosmarinic acid (0.05 mg/mL).

Solvent displacement method constitutes a straightforward and rapid route to the fabrication of nanoparticles by decreasing the quality of the solvent in which a solute (the active ingredient in this case) is dissolved (Joye & McClements, 2013). The nanoparticle formation is instantaneous and the ent3ire procedure is carried out in only one step. Nanoprecipitation occurs by a rapid desolvation of the solute when the solute solution is added to the non-solvent. Indeed, as soon as the solute-containing solvent has diffused into the dispersing medium, the solute precipitates. Several works have reported the entrapment of compounds (drugs, antioxidants, among others) into polymer nanoparticles by solvent displacement method (Bilati, Allémann, & Doelker, 2005; Kakran, Sahoo, Tan, & Li, 2012). It has been found that the particles obtained by nanoprecipitation exhibit better solubility, bioavailability and dispersibility. Despite its advantages, the use of solvent displacement method in food or food packaging applications is still in its infancy.

Recently, we have developed cassava starch films containing aqueous extract of rosemary (Piñeros-Hernandez et al., 2017). The aqueous extract was well incorporated within the starch matrix, despite that some cracks on the films cross-section were formed. Moreover, it was found that the extract presence reduced the bonding between glycerol and starch molecules and thereby, the films showed a strong reduction in their strain at break, while a slight increase in their tensile strength was also observed. In the current work, different concentrations of ethanolic extract (instead an aqueous extract) were incorporated in glycerol-plasticized cassava starch films. Unlike the aqueous extract, the solubility of rosemary active compounds in the ethanol–water mixture was lowered compared to that in the original solvent (ethanol) and in this way, a driving force for precipitation was created. The new composite films were characterized in term of their morphology, surface hydrophobicity, mechanical and barrier properties. Moreover, the release behavior of the rosemary polyphenols from the cassava starch active films to food simulants was studied. To the best of our knowledge, it is the first time that cassava starch films containing rosemary nanoparticles produced by solvent displacement method are developed and characterized for potential food packaging applications.

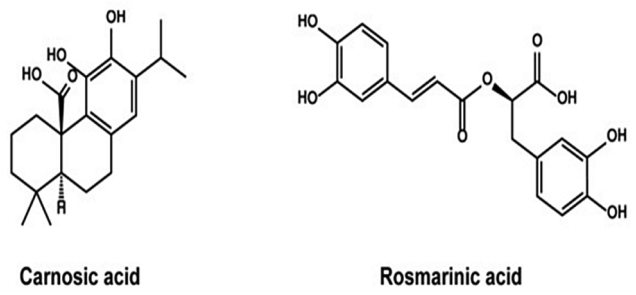

Fig. 1. Chemical structure of major antioxidant compounds present in rosemary extract: rosmarinic and carnosic acid.

2. Materials and methods

2.1. Materials

Cassava starch (18 wt % amylose and 82 wt % amylopectin), provided by Industrias del Maíz S.A (Buenos Aires, Argentina), was used as the film-forming biopolymer. Analytical grade glycerol (Aldrich, USA) was used as plasticizer. Dried and milled rosemary leaves were purchased from a local market in Buenos Aires, Argentina.

2.2. Preparation of ethanolic extract of rosemary

The preparation of the ethanolic extract of rosemary was performed according to optimized protocol reported by Rodríguez-Rojo et al. (2012). A blend containing 10 g of dried and milled rosemary leaves and 100 mL of ethanol 96% was placed in a thermostatic bath at 50 °C for 60 min. Once obtained, the extracts were cooled and filtered (pore size 0.45 μm).

In order to determine the yield of ethanol soluble principle extractions, extract samples (*c.a.* 5 mL) were weighed and oven dried at 80 °C until constant weigh (*c.a.* 24 h). The extraction yield was expressed as grams of dried extract in 100 mL of sample.

2.3. Determination of the total polyphenols content and the antioxidant activity

Total polyphenols content was determined by the Folin-Ciocalteu method (Singleton, Orthofer, & Lamuela-Raventós, 1999). Briefly, 400 μL of each sample were mixed with 2 mL of Folin-Ciocalteu reagent (Anedra, Argentina, 1:10 diluted). Then, 1.6 mL of sodium carbonate (7g/100 mL) (Anedra, Argentina) were added to each sample. After 30 min, the absorbance was measured at 760 nm using spectrophotometer (SHIMADZU UV-1800, Japan). The results were expressed as gallic acid equivalents (GAE).

The polyphenols concentration necessary to reduce the initial amount of DPPH radical to 50%, called efficient concentration (EC_{50}), was determined as reported Brand-Williams, Cuvelier, and Berset (1995). Rosemary extracts were diluted with distilled water in order to reach different polyphenols concentrations. A volume of 100 μL of each sample was mixed with 3.9 mL of 1,1-diphenyl-2-picrylhydrazyl (DPPH•) ethanol solution (25 mg DPPH•/L). Absorbance was determined at 515 nm until the reaction reached a plateau. The DPPH• -scavenging activity of each sample was expressed as the inhibition percentage calculated with the following equation:

$$\text{DPPH}\cdot\text{inhibition}\ (\%) = ((A_b - A_s)/A_b) \times 100 \quad (1)$$

where A_b is the absorbance of the blank and A_s is the absorbance of the sample.

2.4. Solubility of rosemary polyphenols in solvent–antisolvent systems

The solubility of rosemary polyphenols in different solvent–antisolvent ratios was measured as reported Kakran et al. (2012). Different volumes of rosemary ethanolic extract and distilled water were blended in order to obtain ethanol to water ratios of 1:5 and 1:20 (solvent-antisolvent). The mixtures were shaken continuously at room temperature (25 °C) for 24 h and filtered. The solubility (S) of the rosemary polyphenols in the different solvent-antisolvent ratios was calculated using the following equation:

$$S\ (\%) = \left(\frac{TPC_f}{TPC_i}\right) \times 100 \quad (2)$$

where TPC_i is the total polyphenols content of the ethanolic rosemary extract and TPC_f is the remaining polyphenols content in the water-ethanol solvent system, after precipitation (*i.e.* the solution after filtration).

2.5. Particle size distribution analysis of rosemary nanoparticles

The size of the rosemary nanoparticles was measured with Laser Diffraction Particle Size Analyzer SALD-3101 (Shimadzu, Japan).

2.6. Preparation of films

Cassava starch films were produced by solvent casting process as reported in previous works (García, Famá, Dufresne, Aranguren, & Goyanes, 2009; Medina Jaramillo, González Seligra, Goyanes, Bernal, & Famá, 2015; Seligra, Jaramillo, Famá, & Goyanes, 2016). Cassava starch films (CSF) were prepared based on blends containing cassava starch (5.0 g), glycerol (1.5 g) and distilled water (93.5 g). In order to prepare the cassava starch active films (CSAF), a water mass (5 g or 20 g) from the formulations was replaced with the same amount of ethanolic extract of rosemary. The film formulations, the ethanol to water ratios and the concentration of rosemary polyphenols in the film-forming solutions are shown in Table 1. Each blend was homogenized for 40 min using a magnetic stirrer at a speed about 250 rpm and then heated until 96 °C (heating rate = 3 °C/min), under constant stirring. The formulations were degassed for 7 min with a mechanical vacuum pump, dispensed into polypropylene plates and dried at 50 °C for 24 h. Prior to characterization studies, films were conditioned at room temperature into desiccators containing supersaturated solution of sodium bromide (RH ≈ 57%) for 48 h. The resulting films exhibited thicknesses of around 200 μm and water contents ranging between 13% and 17% (wet basis).

2.7. Microscope observations

Micrographs of surface and cross-sections of the films were obtained using a scanning electron microscope (FE-SEM) (SUPRA 40, Carl Zeiss NTS, Germany). The specimens were cryofractured by immersion in liquid nitrogen. The samples were mounted on stubs and sputtered with a thin layer of gold (thickness below 50 nm) prior to SEM observations. Images at different magnifications (from 2,000× up to 50,000×) were obtained using a voltage of about 3 kV and a spotsize of ~ 2 nm.

2.8. Surface hydrophobicity of the films

The contact angle (θ) was used to estimate the surface hydrophobicity of the films. A 2 μL-droplet of ultrapure water was deposited on the film surface and the image of the drop was recorded with a digital microscope (MicroView, China). The contact angles were measured using the ImageJ free software (Stalder, Kulik, Sage, Barbieri, & Hoffmann, 2006).

2.9. Film barrier properties

Water vapor permeability (WVP) tests were carried out at room temperature following the ASTM E96/ASTM E96M-16 method. Film samples were sealed over a circular opening of 4×10^{-4} m^2 in a permeation cell containing calcium chloride. Then, the cells were placed in desiccators conditioned with sodium chloride saturated solution (75% RH). Changes in the weight of the cell were recorded to the nearest 0.0001 g and plotted as a function of time and the slope of each line was calculated by linear regression. WVP (g Pa^{-1} s^{-1} m^{-1}) was calculated as follows:

$$WVP = \left[\frac{WVTR}{P \times RH}\right] \times d \quad (3)$$

where WVTR is the water vapor transmission rate calculated as the ratio between the slope of the straight line (g/s) and the cell area (m^2); P is the saturation vapor pressure of water (Pa); *RH* is the relative humidity in the desiccator, and *d* is the film thickness (m).

Film transparency was measured by its ability to transmit light in the visible region (Han & Floros, 1997). Films were cut into rectangles (50 mm × 10 mm) and placed on the internal side of a quartz spectrophotometer cell. The percent transmittance (% T) of light at 600 nm (T_{600}) was measured using a UV–visible spectrophotometer (SHIMADZU UV-1800, Japan) and the transparency was calculated as the ratio between $\log T_{600}$ and the thickness (mm) of each film.

2.10. Uniaxial tensile tests

Uniaxial tensile tests were carried out using Instron dynamometer 5982 at a strain rate of 5 mm/min, according to ASTM D882-12 standard. Probes with similar dimensions were used (length: 50 mm, wide: 5 mm and thickness: 0.2 mm) and at least 3 replicates of each film type were tested. Nominal stress–strain curves were obtained and Young's modulus, tensile strength and strain at break were calculated according to ASTM D882-12 standard.

2.11. Fourier transform infrared spectroscopy (FTIR)

FTIR analysis was performed using Nicolet 380 equipment

Table 1
Film formulations, ethanol to water ratios and concentration of rosemary polyphenols in the film-forming solutions.

Labels	Film-forming solution components (g/100 g)				Ethanol:water ratio	mg polyphenols/100 g dry solids
	Starch	glycerol	Water	Ethanolic rosemary extract (RE)		
CSF	5	1.5	93.5	0	–	0
CSAF_5%	5	1.5	88.5	5	1:20	197
CSAF_20%	5	1.5	73.5	20	1:5	754

(Thermo Scientific, USA) equipped with attenuated total reflectance (ATR) module. The samples were placed on the ATR accessory and then were analyzed under transmission mode, taking 64 scans per experiment with a resolution of 4 cm^{-1}. FTIR spectra were normalized with the smallest absorbance set to 0 and the highest to +1.

2.12. Thermogravimetric analysis (TGA)

TGA was performed using SHIMADZU DTG-60 (Japan) equipment. Samples (3.0–5.0 mg) were placed in aluminum pans inside the thermogravimetric balance and then heated under dry nitrogen atmosphere (30 mL/min) in the range of 30–400 °C at a heating rate of 10 °C min^{-1}.

2.13. Film swelling

Swelling index defined by the ratio of the volumes of the films in the dry and swollen states was evaluated. Film disks (diameter ≈16 mm) were immersed in 10 mL of distilled water (pH = 6) and allowed to equilibrate at room temperature for 24 h. Diameters of the dry (D_d) and swollen (D_S) film disks were measured photographically using the Image J software. Swelling index (S_R) was calculated as follows:

$$S_R = (D_d/D_s)^3 \quad (4)$$

2.14. Release studies into food simulants

Release studies were performed using distilled water and ethanol 95% as aqueous and fatty food simulants, respectively (Baner, Bieber, Figge, Franz, & Piringer, 1992).

Films samples (50 mg) were immersed in 5 mL of food simulant and placed in a shaker at 25 °C and 125 rpm. Aliquots of supernatant were removed at different times for 168 h (7 days), and the amount of the rosemary polyphenols dissolved in the withdrawn solution was quantified by the Folin-Ciocalteau method (Section 2.3). The cumulative amount of rosemary polyphenols released from the specimens for each specified immersion period was calculated as follows:

$$\text{Polyphenols released } (\%) = \left(\frac{m_t}{m_\infty}\right) \times 100 \quad (5)$$

where m_t is the mass of polyphenols quantified at each time t and m_∞ is the mass of polyphenols loaded in the films. Both m_t and m_∞ were determined by Folin-Ciocalteu method (Section 2.3).

The fitting of the release profile of rosemary polyphenols into food simulants to the empirical models of power law (Ritger & Peppas, 1987) and diffusion-relaxation (Peppas & Sahlin, 1989) was evaluated using the corrected correlation coefficient (R^2_{cor}) and the residual analysis (SYSTAT software, USA).

2.15. Statistical analysis

The statistical analysis was performed using the Systat Inc. software (Evanston, USA). Assumptions of normality and variance-homogeneity were tested with the Shapiro-Wilk and Levene tests, respectively. Analysis of variance (ANOVA) and Tukey pairwise comparisons were carried out using a level of 95% confidence ($\alpha = 0.05$). The experiments were performed at least in duplicate and the data were reported as mean ± standard deviation.

3. Results and discussion

3.1. Properties of rosemary extract

The extraction yield of ethanol soluble compounds from rosemary leaves was 1.8 g of dried extract/100 mL of sample and the total phenolic content of the ethanolic extract was 2.4 mg of gallic acid equivalents (GAE) per milliliter. With respect to the antioxidant activity, the extracts exhibited an efficient concentration (EC_{50}) around 90.01 ± 0.08 μg GAE/mL. These results are in accordance with previous studies demonstrating excellent antioxidant activity for the ethanolic extract of rosemary due to the high content of phenolic compounds (Rodríguez-Rojo et al., 2012).

On the other hand, the solubility of rosemary polyphenols in different ethanol to water ratios was evaluated. In all cases, the extracts exhibited turbid appearance when they were blended with water and rosemary nanoparticles were formed as it is shown in Fig. 2.

Size distributions of the rosemary nanoparticles obtained with different ethanol to water ratios are shown in Fig. 3. Rosemary nanoparticles obtained with ethanol to water ratio 1:20 showed a narrower size distribution (diameters ≈ 0.1–0.5 μm) than the particles obtained with1:5 ratio (diameters ≈ 0.1–2.0 μm). Moreover, the solubility of the rosemary polyphenols decreased from 90 to 46%, when the concentration of ethanolic rosemary extract went from 5% to 20% w/w, respectively. As it is well known, a precipitation process consists of several stages such as: generation of supersaturation, nucleation, and subsequent growth of nuclei. Generation of supersaturation is a prerequisite for the nucleation to occur. In this case, the use of ethanolic extract at 20 %w/w led to a higher driving force for precipitation.

3.2. Physicochemical properties of the cassava starch active films

Fig. 4 shows SEM images of surface and cross-section of films with and without ethanolic extract of rosemary. Samples CSF showed an ordered and homogeneous structure (i.e. without pores and cracks). In CSAF_5% and CSAF_20% samples rosemary particles were observed in both surface and film cross-sections. As expected, the rapid desolvation of some non-water-soluble extract components (e.g. carnosic acid), when the ethanolic extract was blended

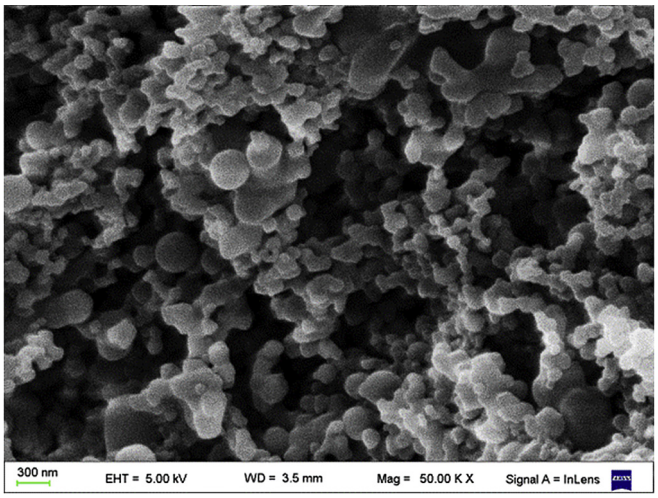

Fig. 2. SEM micrographs of the rosemary nanoparticles obtained by solvent displacement method.

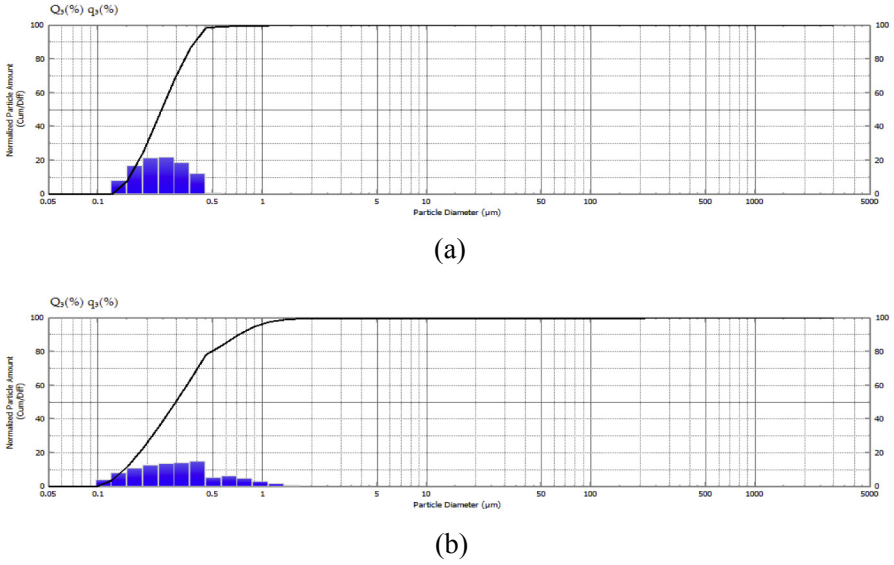

Fig. 3. Size distributions of the rosemary nanoparticles obtained with different ethanol to water ratios: (a) 1:20 and (b) 1:5.

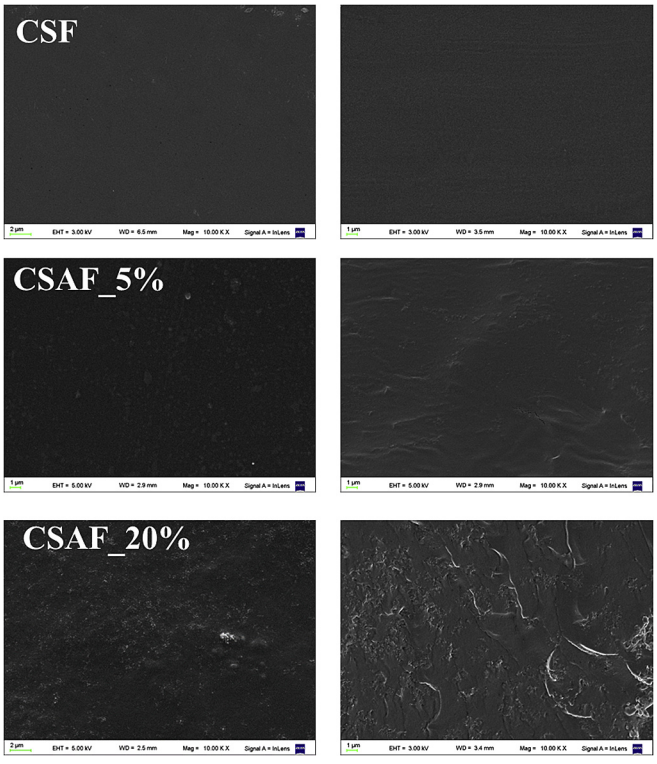

Fig. 4. SEM images of surface and cross-section of films with and without ethanolic extract of rosemary.

with water, led to nanoprecipitation. Gonçalves et al. (2013) stressed that due to the hydrophobic character of some antioxidants, conferred by their hydrocarbon chains, it is conceivable that the precipitation of hydrophobic components occurs. These incompatibilities cause morphological changes in the films (e.g. rougher surface). Similar observations were reported by Pastor, Sánchez-González, Cháfer, Chiralt, and González-Martínez (2010) and Chang-Bravo et al. (2014) when worked on biopolymer films carrying ethanolic extracts of propolis.

The samples added of the lowest concentration of rosemary extract (CSAF_5%) showed a good dispersion of the nanoparticles within the film matrix; while, in the CSAF_20% samples some agglomerates of nanoparticles were observed (Fig. 4). This behavior was attributed to that using a low concentration of extract a more homogeneous particle size distribution was obtained (Fig. 3) and therefore the nanoparticles were better incorporated within the films. Similar observations were reported by Teodoro, Mali, Romero, & de Carvalho, 2015 when worked on the fabrication of cassava starch films containing acetylated starch nanoparticles as reinforcement.

IR spectra of all films showed characteristic bands of cassava starch around 3300 cm^{-1} (O–H stretching), 2947 cm^{-1} (C–H stretching from alkyl groups), 1642 cm^{-1} (H_2O bending vibration), 1455 cm^{-1} (C–H bending), 1242 cm^{-1} (C–O stretching), 1204 cm^{-1} (C–OH stretching), 1149 cm^{-1} (C–O stretching of the –C–O–H), 1103 cm^{-1} (C–O–H stretching), 1076 cm^{-1} (C–O bond stretching of the –C–O–C), 991 cm^{-1} (CH_2 bending) and 925 cm^{-1} (C–O and C–H stretching) (Fig. 5). Other signals around 1042 cm^{-1} and 1015 cm^{-1} were also detected. Similar signals were found by Liu, D., Parker, M. L., Wellner, N., Kirby, A. R., Cross, K., Morris, V. J., & Cheng, F. (2013) when worked on wild type and a ae high-amylose mutant maize kernels. These authors suggested that the bands located about 1042 cm^{-1} and 1015 cm^{-1} can be associated with changes in the short-range order of amylosic helices within the crystal structure.

In order to compare the available amount of OH groups in the different systems, the ratios between the intensities of the peaks at 3300 cm^{-1} (I_{3300}) and at 1149 cm^{-1} (I_{1149}) were calculated. This last signal was chosen as the reference peak assuming that the total number of 'C–O' bonds in 'C–O–H' groups remained the same in the samples with and without RE (Seligra et al., 2016; Shi et al., 2008). In general, the cassava starch active films showed lower I_{3300}/I_{1149} ratio than the films without extract (i.e. lower available amount of OH groups). Moreover, the samples CSAF_20% showed a greater reduction in the OH amount compared with CSF and CSAF_5%. This behavior may be attributed to the RE presence, which interacted with the glycerol-starch matrix resulting in a change of the OH availability within the polymer network (Piñeros-Hernandez et al., 2017).

Fig. 6 shows the TGA curves of the films with and without

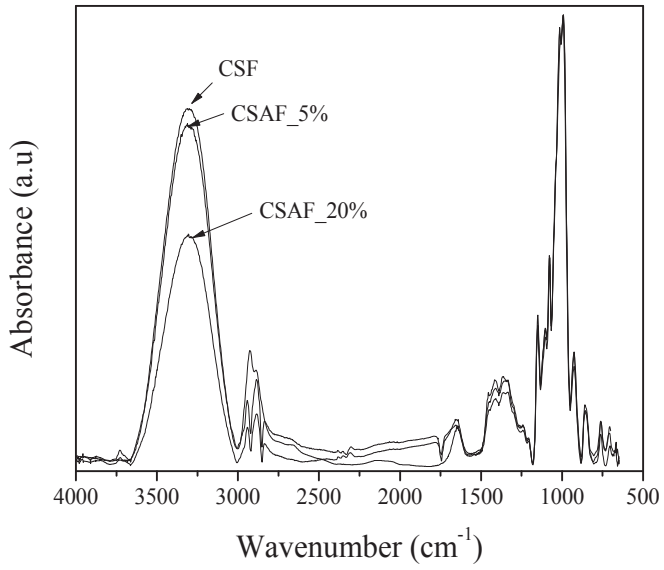

Fig. 5. FTIR spectra of films with and without ethanolic extract of rosemary.

ethanolic extract of rosemary. The thermal degradation of the cassava starch films without extract (CSF) followed the pattern described in the literature typical of glycerol-plasticized starch-films (Nancy L. García et al., 2009). A small step of weight loss (c.a. 10%) between 50 and 150 °C was attributed to water loss. The mass loss event between 200 and 255 °C could be attributed to the decomposition of the glycerol-rich phase. At temperatures higher than 255 °C occurs the oxidation of the partially decomposed starch. In the films carrying RE, the degradation temperatures showed a shift towards lower values, respect to the CSF samples. These results agree with FTIR studies showing that the presence of

Table 2
Barrier properties of the cassava starch films with and without ethanolic extract of rosemary.

Films	WVP (g $s^{-1}m^{-1}Pa^{-1}$ $\times 10^{-10}$)	Transparency (%)
CSF	5.8 ± 0.5[a]	7.44 ± 0.01[a]
CSAF_5%	8.1 ± 1.1[b]	6.82 ± 0.02[b]
CSAF_20%	12.5 ± 1.0[c]	5.47 ± 0.08[c]

Different letters within the same columns indicate statistically significant differences.

extract provoked changes in the conformation of starch polymer.

Surface hydrophobicity of the cassava starch films was not affected by the addition of ethanolic extract of rosemary ($p > 0.05$). Values of contact angles ranging between 34° and 40° were obtained in all cases, which are characteristics of hydrophilic surfaces (Vogler, 1998). Piñeros-Hernandez et al. (2017) reported higher contact angles (49°–53°) for cassava starch films with aqueous extract of rosemary. According to Rodríguez-Rojo et al., 2012 the ethanolic extracts of rosemary are richer in carnosic acid than the aqueous ones. These last extracts are rich in rosmarinic acid and have negligible amounts of carnosic acid. The solubility of carnosic acid in water is much lower than that of rosmarinic acid due to that carnosic acid with two −OH groups and a −COOH group is much more hydrophobic than rosmarinic acid with four −OH groups and a −COOH group (Fig. 1) (Rodríguez-Rojo et al., 2012). Therefore, it could be stated that the nanoprecipitation allowed increasing the hydrophilicity of the films. This behavior could be attributed to the high surface to volume ratio of the rosemary nanoparticles.

With respect to the light barrier properties, all films were clear enough to be used as see-through packaging. However, the cassava starch active films showed lower transparency than the control films (Table 2). Vicentini, Dupuy, Leitzelman, Cereda, & Sobral, 2005 worked on the prediction of cassava starch edible film properties (mechanical, optical, and barrier properties) by chemometric

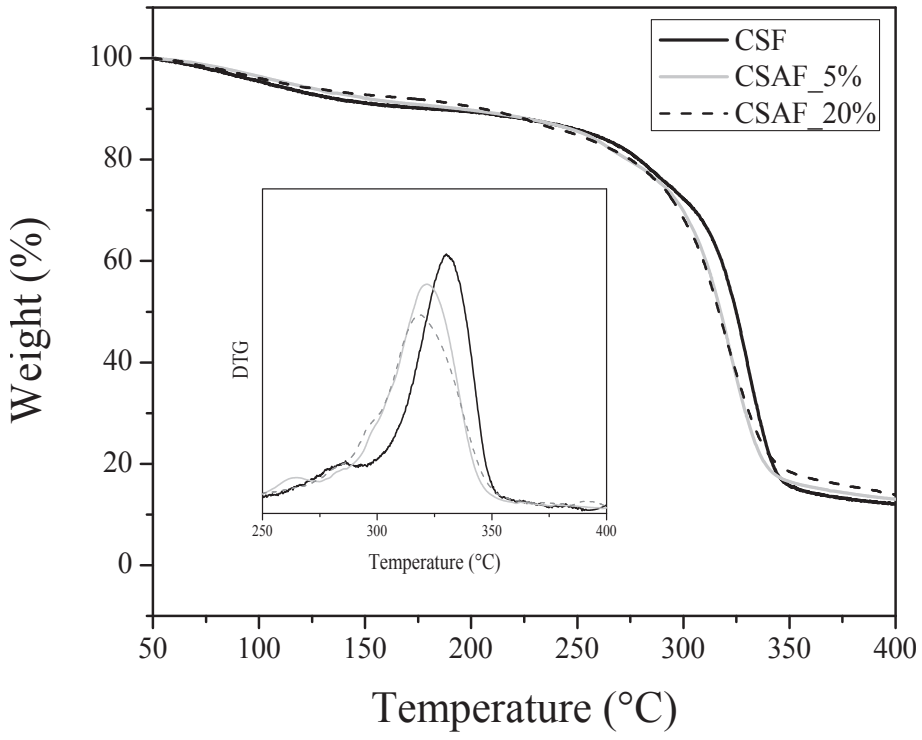

Fig. 6. TGA curves of control films and active films carrying rosemary extract.

analysis of infrared spectra. These authors stressed that if the film properties are related to structural changes in cassava starch films, the infrared spectra must contain some information relative to these modifications. In the current work, the films with lower transparency exhibited a greater reduction in the intensity of the bands located in the 1500-1250 cm^{-1} region (Fig. 5).

The values of water vapor permeability (WVP) of the cassava starch films with and without rosemary extract are shown in Table 2. The cassava starch films containing ethanolic extract of rosemary (CSAF_5% and CSF_20%) showed higher WVP values than the control films (CSF). In particular, the active films containing the greatest concentration of extract (CSF_20%) exhibited WVP values about 2-fold higher compared with the control films (Table 2). This behavior was probably due to the weak polymer–nanoparticle interfacial interaction and to the presence of nanoparticles agglomerates which promoted the transport of water molecules throughout the edible films (Pranoto, Rakshit, & Salokhe, 2005; Sayanjali, Ghanbarzadeh, & Ghiassifar, 2011). In addition, the water vapor transfer could be promoted by the hydrophilic character exhibited by the film surface above discussed.

Fig. 7 shows the stress-strain curves of the films with and without rosemary extract. In general, the presence of rosemary extract led to an increase in the Young's modulus and in the tensile strength of the films. CSFA_5% samples showed values of Young's modulus and of tensile strength about 4.0-fold and 2.5-fold higher compared with the CSF films, respectively. This behavior was attributed to that the rosemary nanoparticles were well distributed within the films and were able to act as a reinforcement of the polymer matrix (Fig. 4). In the case of the films with higher extract amount added, the appearance of larger agglomerates of the nanoparticles in the films provoked a reduction in the strength at break, compared with the CSFA_5% samples (Fig. 4). On the other hand, CSFA_5% and CSFA_20% samples showed a reduction in their strain at break values about 3 and 22%, respectively, compared with the CSF films. Piñeros-Hernandez et al. (2017) when worked on cassava starch films containing aqueous extract of rosemary (instead of ethanolic extract) found that the presence of extract provoked a higher reduction in the values of strain at break, which showed a decrease up to 60%, compared with the films without extract.

3.3. Swelling and release studies

Fig. 8 shows digital images of the films in the dry and swollen states. Control (CSF) and active films (CSAF_5% and CSAF_10%) showed similar values of swelling ratio, about 5. These results suggest that all samples exhibited similar affinity with water. According to Peppas & Khare, 1993 the dynamic swelling behavior of polymer systems can be controlled by the structure of the polymeric network and polymer-solvent interactions. As the dissolution medium penetrates the polymer matrix, the solvent-free polymer starts swelling.

The release kinetics of rosemary polyphenols from cassava starch active films to aqueous and fatty food simulants are shown in Fig. 9. It was found that the differences in the polarity of the food simulants led to changes in the release profile of rosemary polyphenols from the active films. In the aqueous medium, all active films released a polyphenols amount above 60% within the first hour of assay. Therefore, the empirical models of power law and diffusion-relaxation could no longer be applied after 30 min because these models are valid up to 60% release (m_t/m_∞ is < 0.6). The remaining amount of rosemary polyphenols was released within the following 3 h of study reaching plateau overtime. This behavior was not dependent on the initial amount of polyphenols loaded in the films and was attributed to both the high polyphenols affinity to the simulant and the swelling of the films (Fig. 8). These results are in accordance with previous studies deal with the release of hydrophilic compound from polymer matrices (Chang-Bravo et al., 2014).

On the other hand, the release rate of rosemary polyphenols into ethanol (i.e. a fatty food simulant) was slower compared with the aqueous one. A low percentage of recovery of rosemary polyphenols was obtained at 3 h of assay, around 10% and 36% for CSAF_5%, and CSAF_20%, respectively (Fig. 5). After 8 h of assay, the released polyphenols amount from CSAF_5% remained constant overtime; while, polyphenols were quickly released from CSAF_20%

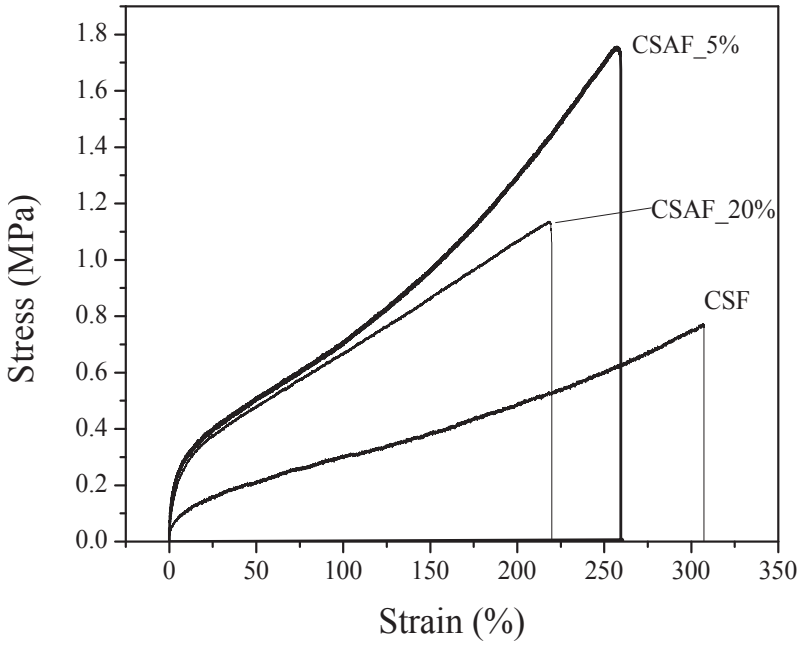

Fig. 7. Stress-strain curves of the films with and without rosemary nanoparticles.

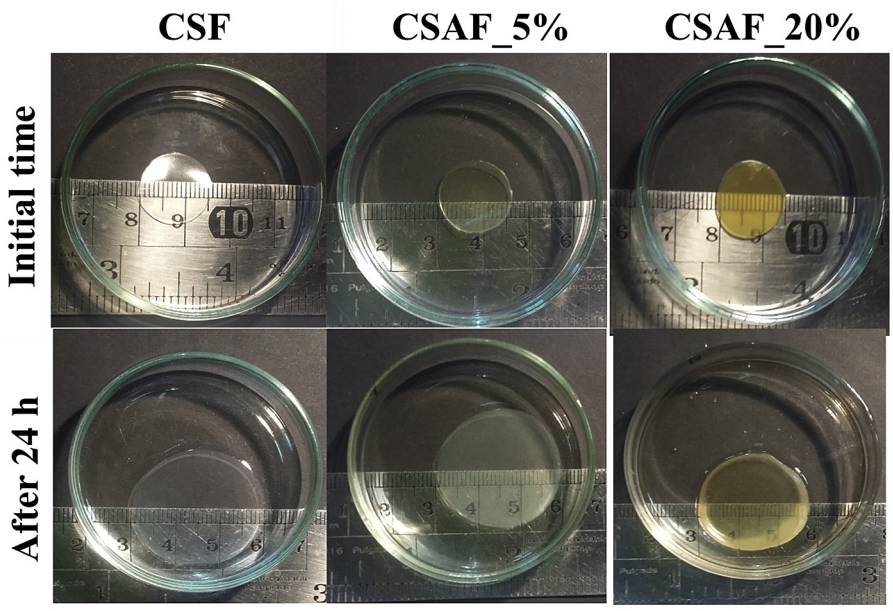

Fig. 8. Swelling behavior of the cassava starch films with and without ethanolic extract of rosemary.

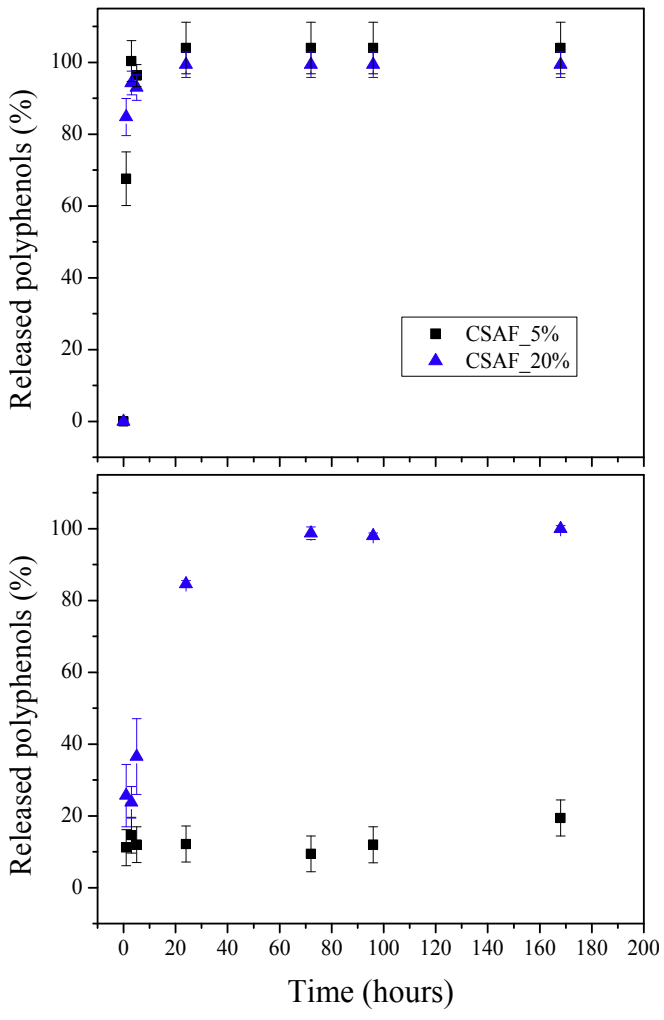

Fig. 9. Release of rosemary polyphenols from cassava starch active films to aqueous and fatty food simulants overtime.

reaching a polyphenol recovery about 100% after 60 h of assay. The fitting of the release profiles of these systems to the models of power law and diffusion-relaxation was unsatisfactory (R^2_{cor} <0.5).

4. Conclusions

The incorporation of ethanolic extracts of rosemary within film-forming aqueous blends containing cassava starch and glycerol proved to be a useful and simple way to produce cassava starch films containing rosemary nanoparticles. The extract amount added to the formulations was an important factor for controlling the driving force for precipitation. The presence of rosemary nanoparticles provoked a strong increase in the elastic modulus and the tensile strength of the films. While, other film properties such as thermal behavior, surface hydrophobicity and swelling were slightly affected. Release studies in food simulants showed that the active films exhibited a sustained release in fatty food simulants along 7-days of assay. Overall, these results suggest that the cassava starch films containing rosemary nanoparticles could find useful applications in food packaging.

Acknowledgements

The authors would like to thank the Consejo Nacional de Investigaciones Cientificas y Tecnicas-Argentina (CONICET, PIP 11220120100508CO), Universidad de Buenos Aires (UBACYT 20020130100495BA) and ANPCyT (PICT 2012- 1093) for their financial support.

References

Aguilar, F., Autrup, H., Barlow, S., Castle, L., Crebelli, R., Dekrant, W., et al. (2008). Use of rosemary extracts as a food additive-Scientific opinion of the panel on food additives, flavourings, processing aids and materials in contact with food. *EFSA Journal, 721*, 1–29.

ASTM D882-12. (2012). *Standard test method for tensile properties of thin plastic sheeting* (16 ed.). West Conshohocken, PA: ASTM International www.astm.org. Last accesed 14/09/2016.

ASTM E96/ E96M-16. (2016). *Standard Test Methods for water vapor transmission of materials* (16 ed.). West Conshohocken, PA: ASTM International www.astm.org. Last accesed 14/09/2016.

Baner, A., Bieber, W., Figge, K., Franz, R., & Piringer, O. (1992). Alternative fatty food simulants for migration testing of polymeric food contact materials. *Food Additives & Contaminants, 9*(2), 137–148.
Bhushani, J. A., & Anandharamakrishnan, C. (2014). Electrospinning and electrospraying techniques: Potential food based applications. *Trends in Food Science & Technology, 38*(1), 21–33.
Bilati, U., Allémann, E., & Doelker, E. (2005). Development of a nanoprecipitation method intended for the entrapment of hydrophilic drugs into nanoparticles. *European Journal of Pharmaceutical Sciences, 24*(1), 67–75.
Brand-Williams, W., Cuvelier, M. E., & Berset, C. (1995). Use of a free radical method to evaluate antioxidant activity. *LWT - Food Science and Technology, 28*(1), 25–30.
Chang-Bravo, L., López-Córdoba, A., & Martino, M. (2014). Biopolymeric matrices made of carrageenan and corn starch for the antioxidant extracts delivery of Cuban red propolis and yerba mate. *Reactive and Functional Polymers, 85*(0), 11–19.
Fabra, M. J., López-Rubio, A., & Lagaron, J. M. (2016). Use of the electrohydrodynamic process to develop active/bioactive bilayer films for food packaging applications. *Food Hydrocolloids, 55*, 11–18.
García, N. L., Famá, L., Dufresne, A., Aranguren, M., & Goyanes, S. (2009). A comparison between the physico-chemical properties of tuber and cereal starches. *Food Research International, 42*(8), 976–982.
García, N. L., Famá, L., D'Accorso, N. B., & Goyanes, S. (2015). Biodegradable starch nanocomposites. In V. K. Thakur, & M. K. Thakur (Eds.), *Eco-friendly polymer nanocomposites* (Vol. 75, pp. 17–77). India: Springer.
Gonçalves, C. M. B., Tomé, L. C., Garcia, H., Brandão, L., Mendes, A. M., & Marrucho, I. M. (2013). Effect of natural and synthetic antioxidants incorporation on the gas permeation properties of poly(lactic acid) films. *Journal of Food Engineering, 116*(2), 562–571.
Han, J. H., & Floros, J. D. (1997). Casting antimicrobial packaging films and measuring their physical properties and antimicrobial activity. *Journal of Plastic Film and Sheeting, 13*(4), 287–298.
Jiménez, A., Fabra, M. J., Talens, P., & Chiralt, A. (2012). Edible and biodegradable starch films: A review. *Food and Bioprocess Technology, 5*(6), 2058–2076.
Joye, I. J., & McClements, D. J. (2013). Production of nanoparticles by anti-solvent precipitation for use in food systems. *Trends in Food Science & Technology, 34*(2), 109–123.
Kakran, M., Sahoo, N. G., Tan, I.-L., & Li, L. (2012). Preparation of nanoparticles of poorly water-soluble antioxidant curcumin by antisolvent precipitation methods. *Journal of Nanoparticle Research, 14*(3), 1–11.
Liu, D., Parker, M. L., Wellner, N., Kirby, A. R., Cross, K., Morris, V. J., et al. (2013). Structural variability between starch granules in wild type and in ae high-amylose mutant maize kernels. *Carbohydrate Polymers, 97*(2), 458–468.
Medina Jaramillo, C., González Seligra, P., Goyanes, S., Bernal, C., & Famá, L. (2015). Biofilms based on cassava starch containing extract of yerba mate as antioxidant and plasticizer. *Starch - Stärke, 67*(9–10), 780–789.
Pastor, C., Sánchez-González, L., Cháfer, M., Chiralt, A., & González-Martínez, C. (2010). Physical and antifungal properties of hydroxypropylmethylcellulose based films containing propolis as affected by moisture content. *Carbohydrate Polymers, 82*(4), 1174–1183.
Peppas, N. A., & Khare, A. R. (1993). Preparation, structure and diffusional behavior of hydrogels in controlled release. *Advanced Drug Delivery Reviews, 11*(1), 1–35.
Peppas, N. A., & Sahlin, J. J. (1989). A simple equation for the description of solute release. III. Coupling of diffusion and relaxation. *International Journal of Pharmaceutics, 57*(2), 169–172.
Piñeros-Hernandez, D., Medina-Jaramillo, C., López-Córdoba, A., & Goyanes, S. (2017). Edible cassava starch films carrying rosemary antioxidant extracts for potential use as active food packaging. *Food Hydrocolloids, 63*, 488–495.
Pranoto, Y., Rakshit, S., & Salokhe, V. (2005). Enhancing antimicrobial activity of chitosan films by incorporating garlic oil, potassium sorbate and nisin. *LWT-Food Science and Technology, 38*(8), 859–865.
Ribeiro, A., Caleja, C., Barros, L., Santos-Buelga, C., Barreiro, M. F., & Ferreira, I. C. F. R. (2016). Rosemary extracts in functional foods: Extraction, chemical characterization and incorporation of free and microencapsulated forms in cottage cheese. *Food & Function, 7*(5), 2185–2196.
Ritger, P. L., & Peppas, N. A. (1987). A simple equation for description of solute release II. Fickian and anomalous release from swellable devices. *Journal of Controlled Release, 5*(1), 37–42.
Rodríguez-Rojo, S., Visentin, A., Maestri, D., & Cocero, M. J. (2012). Assisted extraction of rosemary antioxidants with green solvents. *Journal of Food Engineering, 109*(1), 98–103.
Sayanjali, S., Ghanbarzadeh, B., & Ghiassifar, S. (2011). Evaluation of antimicrobial and physical properties of edible film based on carboxymethyl cellulose containing potassium sorbate on some mycotoxigenic Aspergillus species in fresh pistachios. *LWT-Food Science and Technology, 44*(4), 1133–1138.
Seligra, P. G., Medina Jaramillo, C., Famá, L., & Goyanes, S. (2016). Biodegradable and non-retrogradable eco-films based on starch–glycerol with citric acid as cross linking agent. *Carbohydrate Polymers, 138*, 66–74.
Shi, R., Bi, J., Zhang, Z., Zhu, A., Chen, D., Zhou, X., et al. (2008). The effect of citric acid on the structural properties and cytotoxicity of the polyvinyl alcohol/starch films when molding at high temperature. *Carbohydrate Polymers, 74*(4), 763–770.
Singleton, V. L., Orthofer, R., & Lamuela-Raventós, R. M. (1999). Analysis of total phenols and other oxidation substrates and antioxidants by means of folin-ciocalteu reagent. In P. Lester (Ed.), *Methods in enzymology* (Vol. 299, pp. 152–178). Academic Press.
Stalder, A., Kulik, G., Sage, D., Barbieri, L., & Hoffmann, P. (2006). A snake-based approach to accurate determination of both contact points and contact angles. *Colloids and Surfaces A: Physicochemical and Engineering Aspects, 286*(1), 92–103.
Teodoro, A. P., Mali, S., Romero, N., & de Carvalho, G. M. (2015). Cassava starch films containing acetylated starch nanoparticles as reinforcement: Physical and mechanical characterization. *Carbohydrate Polymers, 126*, 9–16.
Vicentini, N. M., Dupuy, N., Leitzelman, M., Cereda, M. P., & Sobral, P. J. A. (2005). Prediction of cassava starch edible film properties by chemometric analysis of infrared spectra. *Spectroscopy Letters, 38*(6), 749–767.
Vogler, E. A. (1998). Structure and reactivity of water at biomaterial surfaces. *Advances in Colloid and Interface Science, 74*(1), 69–117.